Experimental investigation of dynamic effects in capillary pressure: Grain size dependency and upscaling

Geremy Camps-Roach,[1] Denis M. O'Carroll,[1] Timothy A. Newson,[1] Toshihiro Sakaki,[2] and Tissa H. Illangasekare[2]

Received 6 November 2009; revised 1 April 2010; accepted 5 April 2010; published 31 August 2010.

[1] The macroscopic flow equations used to predict two-phase flow typically utilizes a capillary pressure-saturation relationship determined under equilibrium conditions. Theoretical reasoning, experimental evidence, and numerical modeling results have indicated that when one fluid phase replaces another fluid, this relationship may not be unique but may depend on the rate at which the phase saturations change in response to changes in phase pressures. This nonuniqueness likely depends on a variety of factors including soil-fluid properties and possibly physical scale. To quantify this dependency experimentally, direct measurements of equilibrium and dynamic capillary pressure-saturation relationships were developed for two Ottawa sands with different grain sizes using a 20 cm long column. A number of replicate air-water experiments were conducted to facilitate statistical comparison of capillary pressure-saturation relationships. Water and air pressures and phase saturations were measured at three different vertical locations in the sand column under different desaturation rates (1) to measure local capillary pressure-saturation relationships (static and dynamic); (2) to quantify the dynamic coefficient τ, a measure of the magnitude of observed dynamic effects, as a function of water saturation for different grain sizes and desaturation rates; (3) to investigate the importance of grain size on measured dynamic effects; and (4) to assess the importance of sample scale on the magnitude of dynamic effects in capillary pressure. A comparison of the static and dynamic P_c-S_w relationships showed that at a given water saturation, capillary pressure measured under transient water drainage conditions is statistically larger than capillary pressure measured under equilibrium or static conditions, consistent with thermodynamic theory. The dynamic coefficient τ, used in the expression relating the static and dynamic capillary pressures to the desaturation rate was dependant on porous media mean grain size but not on the desaturation rate. Results also suggest that the magnitude of the dynamic coefficient did not increase with the increased averaging volume considered in this study, as has been reported in the literature. This work suggests that dynamic effects in capillary pressure should be included in numerical models used to predict multiphase flow in systems when saturations change rapidly, particularly in fine-grained soil systems (e.g., CO_2 sequestration, enhanced oil recovery, air sparging for remediation).

Citation: Camps-Roach, G., D. M. O'Carroll, T. A. Newson, T. Sakaki, and T. H. Illangasekare (2010), Experimental investigation of dynamic effects in capillary pressure: Grain size dependency and upscaling, *Water Resour. Res.*, *46*, W08544, doi:10.1029/2009WR008881.

1. Introduction

[2] An understanding of multiphase flow processes is important in many natural and engineered systems including crop irrigation management practices, groundwater remediation and petroleum reservoir engineering. In these systems, under natural or imposed boundary conditions or stresses, there are numerous instances when the rate of saturation change is significant as determined by transient boundary conditions and source conditions. For example, significant rates of saturation change may be expected when injecting CO_2 into deep subsurface aquifers (sequestration reservoirs), water flooding of petroleum reservoirs for oil recovery [*Kalaydjian*, 1992], high pressure sand filter systems and heavy rainfall/irrigation events on soils at residual saturation [*Manthey*, 2006]. Accurate representation of the constitutive relationships between capillary pressure and saturation in predictive models of multiphase flow in these instances is essential.

[3] The capillary pressure-saturation relationship (hereinafter referred to as P_c-S_w relationship) is a basic constitutive

[1]Department of Civil and Environmental Engineering, University of Western Ontario, London, Ontario, Canada.
[2]Center for Experimental Study of Subsurface Environmental Processes, Colorado School of Mines, Golden, Colorado, USA.

0043-1397/10/2009WR008881

relationship that is required for the prediction of multiphase flow behavior in porous media systems. Experimental measurement of the capillary pressure-saturation relationship typically takes weeks or months and data points are usually only quantified under equilibrium conditions (i.e., measurements made after the fluid flow has completely ceased). In standard practice, these capillary pressure-saturation relationships are then applied to nonequilibrium conditions with fluids sometimes flowing at high flow rates. The application of capillary pressure-saturation relationships derived under equilibrium conditions to systems that are far from equilibrium implicitly assumes that disturbances to interfacial properties (e.g., contact angle) are rapidly dissipated [*Hassanizadeh et al.*, 2002]. In a wide range of practical situations of multiphase fluid flow this assumption may be violated.

[4] Although it is commonly assumed that the capillary pressure-saturation relationship is not a function of the desaturation rate, many studies suggest that this may not be the case [e.g., *Topp et al.*, 1967; *Stauffer*, 1978; *Kalaydjian*, 1992; *Schultze et al.*, 1997; *Hassanizadeh et al.*, 2002; *Bottero et al.*, 2006; *Sakaki et al.*, 2010]. For example, air-water drainage experiments conducted by *Topp et al.* [1967] found that capillary pressure, at a given saturation, increased with the rate of desaturation. Similar results have been reported for two phase experiments with tetrachloroethene (PCE) and water [*Berentsen et al.*, 2006; *Bottero et al.*, 2006].

[5] To account for the transient or dynamic effects on the capillary pressure-saturation relationship, *Barenblatt* [1971], *Stauffer* [1978], *Hassanizadeh and Gray* [1990] and *Kalaydjian* [1992] proposed relationships to account for the observed nonuniqueness in the P_c-S_w relationship. The studies of *Hassanizadeh and Gray* [1990] and *Kalaydjian* [1992] used conservation of mass, momentum and energy to develop macroscopic multiphase flow equations. A constitutive relationship for capillary pressure was therefore developed at the REV scale establishing a thermodynamic basis for the concept of dynamic effects in capillary pressure. These studies proposed that the difference between the nonwetting and wetting phase fluid pressures is a function of the capillary pressure measured under static conditions as well as the product of the desaturation rate and a dynamic coefficient (τ) [*Hassanizadeh and Gray*, 1990; *Kalaydjian*, 1992]:

$$P_{NW} - P_W = P_c^{static} - \tau\left(\partial S_w/\partial t\right) \tag{1}$$

where P_c^{static} is the capillary pressure when there are no changes in saturation, P_{NW} is the nonwetting phase pressure measured at any time (i.e., with or without changes in saturation), P_W is the wetting phase pressure measured at any time and $\partial S_w/\partial t$ is the rate of water saturation change.

[6] *Stauffer* [1978] proposed an empirical relationship relating readily measurable porous media and fluid properties, including permeability, to the magnitude of τ:

$$\tau \propto \frac{\phi\mu}{k\lambda}\left(\frac{P_d}{\rho_g}\right)^2 \tag{2}$$

where ϕ is porosity, k is intrinsic permeability, λ and P_d are Brooks-Corey constitutive model parameters (equation (3)) [*Brooks and Corey*, 1964], μ is fluid viscosity, ρ is the fluid density, and g is gravity. Where the Brooks-Corey constitutive model [*Brooks and Corey*, 1964] is

$$P_c = P_d S_w^{eff^{-1/\lambda}} \tag{3}$$

where S_w^{eff} is the effective saturation.

[7] In the model of *Barenblatt* [1971], the capillary pressure and relative permeability relationships under nonequilibrium conditions are determined using an expected *future* water saturation (i.e., a lower water saturation on drainage and a larger water saturation on imbibition for a given capillary pressure). As such his theory suggests that dynamic effects in capillary pressure are related to the finite time required for fluids in the pore structure to rearrange [*Barenblatt*, 1971; *Barenblatt et al.*, 2003; *Juanes*, 2008]. The difference between the current and future saturations is a function of the desaturation rate and is related to a redistribution time. Using a first order approximation the dynamic coefficient can therefore be related to a characteristic redistribution time as [*Juanes*, 2008]

$$\tau(S_w) = \frac{dP_c^{static}}{dS_w} \cdot T_B(S_w) \tag{4}$$

where τ is the dynamic coefficient determined in equation (1) and T_B is the redistribution time. All of these relationships suggest that dynamic capillary pressure, defined as the capillary pressure measured under nonequilibrium conditions, is larger than the static capillary pressure measured under equilibrium conditions, on water drainage and smaller on water imbibition.

[8] The need to include the dynamic coefficient and desaturation rate in the mass balance equations governing multiphase flow has been the subject of some debate in the literature. For example, *O'Carroll et al.* [2005] found that the inclusion of a dynamic capillary pressure term improved the agreement between observed and simulated outflow in PCE-water multiphase outflow experiments. However, studies conducted in air-water systems suggest that the inclusion of a dynamic capillary pressure term was either unnecessary to achieve reasonable agreement between experimental and simulated outflow [*Vogel et al.*, 2008] or only resulted in a slight improvement [*Sakaki et al.*, 2010]. The study of *Sakaki et al.* [2010] found the capillary pressure-saturation relationship, measured under nonequilibrium conditions in both drainage and wetting cycles, was statistically different than that measured under equilibrium conditions for the single soil that was tested. The study of *Vogel et al.* [2008] did not, however, measure the capillary pressure–saturation in situ and therefore could not directly detect if dynamic effects in capillary pressure were present for the conditions of their study. This suggests that although dynamic capillary pressure–saturation effects were quantified, the instances when these effects need to be incorporated in multiphase flow simulators are unclear.

[9] The actual physical mechanisms that result in an increased relaxation (redistribution) time for system equilibrium or the dynamic coefficient (τ) are not clearly understood [*Manthey et al.*, 2008]. Essentially, any factor which increases the time needed to achieve equilibrium increases the magnitude of the dynamic coefficient [*Juanes*, 2008]. Some of the factors that may result in dynamic effects in capillary pressure include imposed boundary conditions [*Manthey*,

Table 1. Soil Properties

Sand Type	k (m^2)	P^d (cm of water)	λ	d_{50} (mm)	U_c
F32/F50	5.3×10^{-11}	22.5	2.7	0.42	2.3
F70	1.47×10^{-11}	47.0	3.9	0.18	1.6

2006], soil properties [*Stauffer*, 1978], dynamic contact angle [*Friedman*, 1999], fluid properties [*Das et al.*, 2007], air and water entrapment, pore water blockage and air entry value effect [*Wildenschild et al.*, 2001] as well as macro and microscale heterogeneities [*Manthey et al.*, 2005; *Mirzaei and Das*, 2007]. According to a review of a number of published studies that were performed over the last five decades [*Hassanizadeh et al.*, 2002], finer textured soils did not consistently result in a larger dynamic coefficient, as would be expected based on equation (2). This suggests that the impact of grain size on observed dynamic effects is still unclear and merits further investigation.

[10] The studies of *Manthey et al.* [2005], *Mirzaei and Das* [2007], and *Das et al.* [2007] are based on numerical modeling and did not include the dynamic coefficient in their governing equations. In these studies they started by assuming that $\tau = 0$ at the point scale. Pressures and saturations were then averaged over their model domain, which was less than 100 cm, and the dynamic coefficient was found to be nonzero by fitting a straight line to the difference in capillary pressure versus desaturation rate (equation (1)). As such they investigated if dynamic effects in capillary pressure were due to upscaling pressure and saturation from the point scale to the domain scale in a numerical model. A number of numerical and theoretical studies investigating the impact of the domain size over which parameters are averaged have suggested that τ is proportional to the square of the length scale [*Dahle et al.*, 2005; *Manthey et al.*, 2005; *Nordbotten et al.*, 2008]. For example *Manthey et al.* [2005] simulated nonequilibrium experiments at varying length scales. Their results showed that as the domain size increased, the difference between the averaged dynamic and static P_c increased while the saturation rate (determined from the averaged saturations) decreased, thereby increasing τ at larger domain sizes. In their study they found that the magnitude of the dynamic coefficient increased from approximately 10^2 kg m^{-1} s^{-1}, with a domain size of 3 cm, to approximately 10^5 kg $m^{-1}s^{-1}$, with a domain size of 100 cm. However, such upscaling effects in τ have not been confirmed experimentally.

[11] Experimental studies in the literature [e.g., *Topp et al.*, 1967; *Berentsen et al.*, 2006; *Bottero et al.*, 2006; *Sakaki et al.*, 2010] have focused on detecting dynamic effects in a single soil and fluid pair system and did not, in a systematic fashion, investigate the impact of other system parameters (e.g., soil and fluid properties) on the dynamic coefficient. Furthermore capillary pressure and saturation that are typically measured at only one location in experimental studies are used to evaluate local dynamic effects. As a result it has not been possible to determine if upscaling pressures and saturations leads to the dynamic effects that have been reported in numerical modeling studies.

[12] In this work, air-water primary drainage capillary pressure-saturation relationships were measured for medium and fine textured sands at three measurement elevations in the same vertical column at a number of different imposed boundary conditions. Water pressure and saturation were quantified at all measurement locations and air pressure was measured at the measurement location in many of the experiments. This approach facilitated the determination of 95% confidence intervals of the capillary pressure–saturation curves measured under both static and dynamic conditions, for the very first time to our best knowledge, to determine if water desaturation rate impacted the magnitude of measured capillary pressure. Using the experimentally measured P_c-S_w relationships, the dynamic coefficient τ was first quantified at point locations. The dependency of grain size (i.e., impacting both intrinsic permeability and entry pressure) on the magnitude of the dynamic coefficient τ was then assessed. Finally, the locally evaluated τ was upscaled over a 9 cm interval of the column length, by averaging pressures and saturations, facilitating an assessment of the impact of upscaling on the dynamic coefficient.

2. Materials and Methods

2.1. Sand Materials

[13] The solid phase used in these experiments was either F32/F50 Ottawa sand (i.e., a 1:1 by weight mixture of F35 and F50 sand) or F70 Ottawa sand (Opta Minerals Inc., Brantford, Ontario, Canada). The F32/F50 sand mixture has a mean grain size of 0.42 mm and a uniformity index of 2.3 (Table 1). The F70 sand has a mean grain size of 0.18 mm and a uniformity index of 1.6.

2.2. Experimental Setup

[14] All experiments were conducted in a custom built aluminum column 20 cm in length with an internal diameter of 10 cm. A set of probes consisting of one nonwetting phase tensiometer, one wetting phase tensiometer and one soil moisture probe was installed at depths of 7 cm (level 1), 10 cm (level 2) and 13 cm (level 3), measured from the upper end of the soil chamber (Figure 1).

[15] Wetting phase tensiometers were developed by connecting ceramic porous cups (0652X03-B1M3, Soilmoisture Equipment Corp., Santa Barbara, California) to FP2000 pressure transducers (Honeywell, Columbus, Ohio).

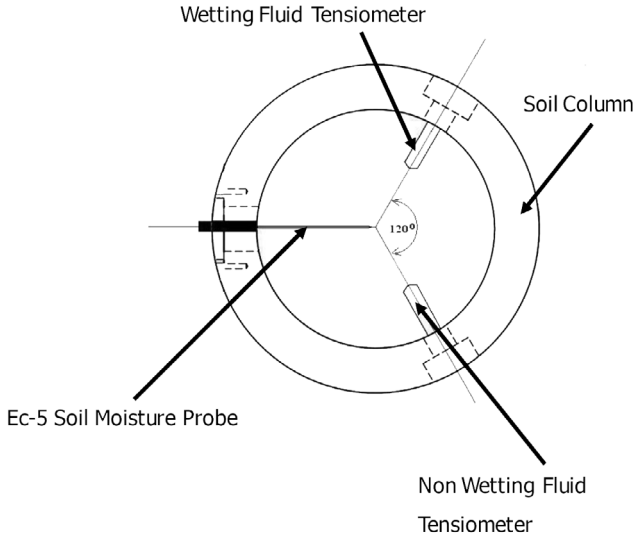

Figure 1. Cross-sectional view of the soil chamber.

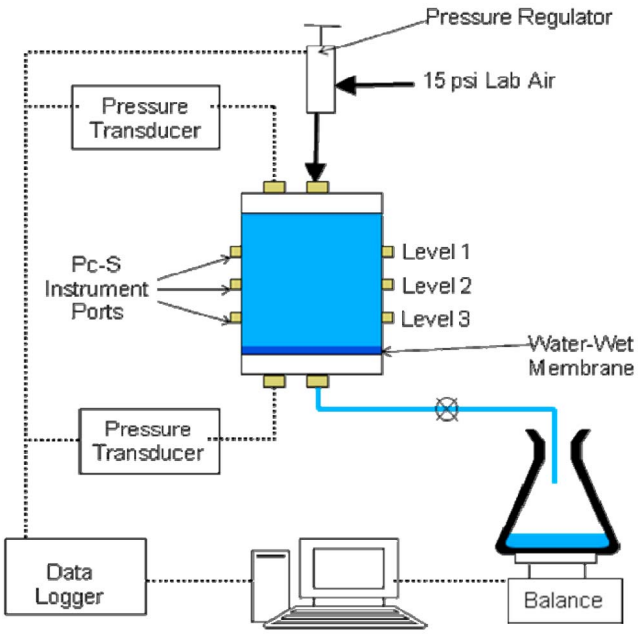

Figure 2. Experimental outflow setup.

Nonwetting phase tensiometers (NWPT) were developed by treating the ceramic cups with a 15% solution (by volume) of Mythyltrichlorosilane (100%) (Sigma-Aldrich Co., Oakville, Ontario) in toluene (100%) [*Sah et al.*, 2004], for 24 h, followed by rinsing thoroughly with methanol (100%). The NWPTs were then air-dried over night before being attached to the pressure transducers. The pressure transducers were connected to a CR7 data logger (Campbell Scientific, Logan, Utah). The wetting and nonwetting phase tensiometers responded to changes in pressure within the measurement interval of the data logger (i.e., 15 s) at 100% water saturation and the water pressure sensors increased to 90% of their steady state value within 90 s and to 95% of their steady state value within 120 s under partially saturated conditions. In this assessment of pressure sensor response time the air inflow line was closed, the outflow water reservoir elevation instantaneously increased, and the time required for the pressure transducers to read this change quantified at the three measurement locations. As such this test assesses the time required for pressure changes at the base of the column to travel through the aqueous phase in the porous media, through the water saturated ceramic porous cup and be read by the pressure transducer. The pressure transducers were calibrated prior to both permeability and outflow experiments to ensure minimal drift (<2 mm) in the readings over the experimental time period.

[16] In the F32/F50 experiments only the upper boundary air pressure was quantified, assuming that the air phase had an infinite mobility, and the upper boundary air phase pressure was used to approximate air phase pressure throughout the column [*Hopmans et al.*, 1996]. In the F70 experiments, air pressure was measured at three locations using the nonwetting phase tensiometers except for one F70 experiment in which the nonwetting fluid phase tensiometer failed (i.e., the ceramic was not adequately hydrophobic). For this experiment, the upper boundary air pressure was used to calculate capillary pressure at levels 1, 2 and 3. In the F70 experiments where the nonwetting fluid tensiometers worked properly and in a separate F32/F50 experiment, the assumption that the air pressure measured at the upper boundary was equal to the air pressure measured at the different depths in the column was confirmed.

[17] Water saturation was determined by soil moisture probes (ECH_2O EC-5, Decagon Devices, Pullman, Washington), whose two prongs were oriented vertically in the column. The sampling height of the EC-5 probes can be taken approximately as 1.0 cm when the plus prong (with EC-5 logo) is placed on top of the shield prong and the drainage front propagates from top to bottom, as adopted in this study [*Limsuwat et al.*, 2009]. The EC-5 probe uses the capacitance technique to measure the dielectric permittivity of porous media [*Czarnomski et al.*, 2005] and responded immediately to changes in water saturation. A two-point calibration procedure was used to calibrate the EC-5 probes [*Sakaki et al.*, 2008]. *Sakaki et al.* [2008] determined an instrument error of less than ± 0.005 cm^3 cm^{-3} for dry sand and ± 0.028 cm^3 cm^{-3} for saturated sand with instrument specific calibration. The EC-5 detection limit (0.7% water saturation) was assumed to be the 95% confidence interval of at least 100 EC-5 readings at 100% water saturation.

[18] Once the tensiometers and EC-5 probes were calibrated and installed, the column was dry packed, and flushed with CO_2 for 20 min. After flushing with CO_2, the column was slowly saturated with de-ionized water vertically upwards at a rate of 1 mL/min for at least 24 h [*O'Carroll et al.*, 2005]. After packing the permeability of the sand was determined at 100% water saturation using a constant head method [*Klute and Dirksen*, 1986]. For experiments with F32/F50 sand, a water saturated hydrophilic membrane (Nylaflo 0.2 μm pore size, Pall Corporation, Ann Arbor Michigan) was placed at the lower end of the pressure cell. In these cases the membrane permeability was determined from experimental data by applying Darcy's law for flow in series. De-ionized water was used as the aqueous phase in all experiments.

2.3. Static and Dynamic Drainage Experiments

[19] Static and dynamic primary drainage experiments were conducted using an automated laboratory apparatus (Figure 2). Outflow was induced by increasing the upper boundary air pressure (P_{air}) above atmospheric pressure. Here, P_{air} was controlled by a pressure regulator attached to a stepping motor. Cumulative outflow (gravimetric), quantified using a balance (Adventure Pro., Ohaus, New Jersey) connected to a computer, water saturations and tensiometric air and water pressures were recorded at 15 s intervals.

[20] In the static experiments air phase pressure was increased in small increments (2–3 cm water) with sufficient time between steps to allow the system to equilibrate (i.e., an outflow rate of <0.2 g/h). Once equilibrium was achieved, this process was repeated until the residual water saturation of the sand was reached. Dynamic experiments were conducted by increasing the P_{air} to either 135 or 214 cm of water in one step. This large initial step ensures a rapid rate of saturation change. All experiments were conducted at a temperature of 22°C (±2°C) in a temperature controlled environmental laboratory.

[21] For the F32/F50 sand, a total of nine drainage experiments were performed under three desaturation rate

Table 2. Summary of Column Parameters After Packing

Sand Type	Static or Dynamic	Imposed Air Pressure (cm of water)	Levels Used to Calculate P_c-S	Porosity ϕ	k_{sand} (m^2)	k_{mem} (m^2)	Cumulative Outflow (g)
F32–F50	Static	n/a	1, 2 and 3	0.32	6.32×10^{-11}	1.15×10^{-15}	361.0[a]
F32–F50	Static	n/a	1, 2 and 3	0.32	6.06×10^{-11}	1.09×10^{-15}	446.0
F32–F50	Dynamic	135	3	0.32	-	-	467.0
F32–F50	Dynamic	135	3	0.32	5.26×10^{-11}	1.07×10^{-15}	461.7
F32–F50	Dynamic	135	3	0.32	2.67×10^{-11}	8.76×10^{-16}	453.4
F32–F50	Dynamic	135	2 and 3	0.32	5.61×10^{-11}	1.50×10^{-15}	469.6
F32–F50	Dynamic	214	2	0.31	-	-	467.3
F32–F50	Dynamic	214	1, 2 and 3	0.31	-	-	444.5
F32–F50	Dynamic	214	2 and 3	0.33	-	-	443.2
Mean			-	0.32	5.18×10^{-11}	1.14×10^{-15}	456.6
Normalized 95% C.I.[b]			-	1.34	7.2	16.0	1.9
F70	Static	n/a	1, 2 and 3	0.32	-	NA	390.2
F70	Static	n/a	1, 2 and 3	0.32	-	NA	379.9
F70	Dynamic	135	1, 2 and 3	0.32	-	NA	365.9
F70	Dynamic	135	1, 2 and 3	0.32	-	NA	376.7
F70	Dynamic	135	1, 2 and 3	0.32	-	NA	368.3
Mean			-	0.32	-	NA	376.2
Normalized 95% C.I.[b]			-	0.7	-	NA	2.7

[a]Experiment stopped before S_{rw} achieved as data acquisition system failed. This reading was not used to compute the mean cumulative outflow.
[b]Normalized 95% C.C. = (95% C.I.)/mean × 100.

regimes. Two experiments were conducted under static or slow desaturation rates. Four experiments were conducted at an intermediate desaturation rate induced by maintaining a constant upper boundary air pressure of 135 cm water and three experiments were conducted at a fast desaturation rate induced by imposing a constant upper boundary air pressure of 214 cm water. For the F70 sand, two static and three dynamic experiments were conducted. The F70 sand dynamic experiments used an upper boundary air pressure of 135 cm water (Table 2). In some instances the tensiometers or soil moisture sensors failed (e.g., the porous ceramic developed a leak allowing water to infiltrate an air pressure line or EC-5 probes failed) and results from this measurement location are not reported.

3. Results and Discussion

3.1. Statistical Analysis of the Measured P_c-S_w Relationships

[22] For each static experiment, the column was packed with either the F32/F50 or F70 sand. Variations in independently quantified porosity and permeability in each experiment were small (i.e., less than 5% for permeability; see Table 2). The P_c-S_w relationship was measured at the three measurement locations (levels 1–3). In the P_c-S_w experiments water drained sequentially starting at level 1 followed by level 2 and then level 3, as shown in Figure 3. The measured static P_c-S_w curves for the F32/F50 and F70 sands were reproducible indicating that a homogeneous and reproducible packing was achieved within the columns. For example Figure 4 presents P_c-S_w data for a dynamic F32/F50 experiment (P_{air} = 214 cm water) in one sand pack at each of the three measurement locations. The entry pressure is very reproducible, similar to the static experiment, and the difference between the three measured capillary pressures, at the same water saturation, are small. Similar reproducibility was observed for other static and dynamic experiments.

[23] To assess the reproducibility of measured P_c-S_w data and to compare measured P_c-S_w data at the different imposed boundary conditions, 95% confidence intervals about the mean static P_c-S_w data were determined for each sand type. To do this the water saturation was divided into 0.005 intervals for static experiments (0.01 intervals for dynamic experiments) and the mean measured capillary pressures and 95% confidence intervals were quantified in this water saturation interval. The data was binned into intervals in this manner as capillary pressures were measured at slightly different water saturations making it difficult to directly compare capillary pressure data at a given measured water saturation. For the static P_c-S_w curves for the F32/F50 sand, 95% confidence intervals of the mean were less than 1.4 cm water for water saturations less than 0.98. In general, the 95% confidence intervals decreased with decreasing water saturation (Figure 5). With the finer F70 sand the 95% confidence intervals were larger but generally less than 2 cm of water (Figure 6). The 95% confidence intervals were larger for the dynamic experiments (Figures 5 and 6). Maximum 95% confidence intervals were 1.6 cm of water for the F32/F50 sand at both imposed boundary conditions and 2.3 cm water, at water saturations below 90%, for the dynamic experiments conducted in the F70 sand.

[24] The capillary pressures measured under dynamic conditions were consistently larger than those measured under static conditions. For the F32/F50 sand, measured capillary pressures were largest at the largest imposed pressure step (214 cm water), followed by the imposed boundary condition of 135 cm water and finally the static condition (i.e., $P_c^{static} < P_c^{135\ cm\ water} < P_c^{214\ cm\ water}$ at a given S_w). The mean entry pressure (P_d) increased with the desaturation rate. For the F32/F50 sand, a mean P_d of 18.1 cm (95% C.I. = 1.6), 23.0 cm (95% C.I. = 0.89) and 26.0 cm (C.I. = 3.1) was recorded for experiments conducted at the slowest (static), intermediate (P_{air} = 135 cm) and fastest (P_{air} = 214 cm) desaturation rates, respectively. These entry pressures are taken as the capillary pressure at the onset of desaturation (S_w = 0.99). The 95% confidence interval of the mean static P_c-S_w curve overlaps with the 95% confidence interval of the P_c-S_w curve measured at the imposed boundary condition of 135 cm water for the F32/F50 sand however at the larger imposed boundary condition the confidence intervals do not

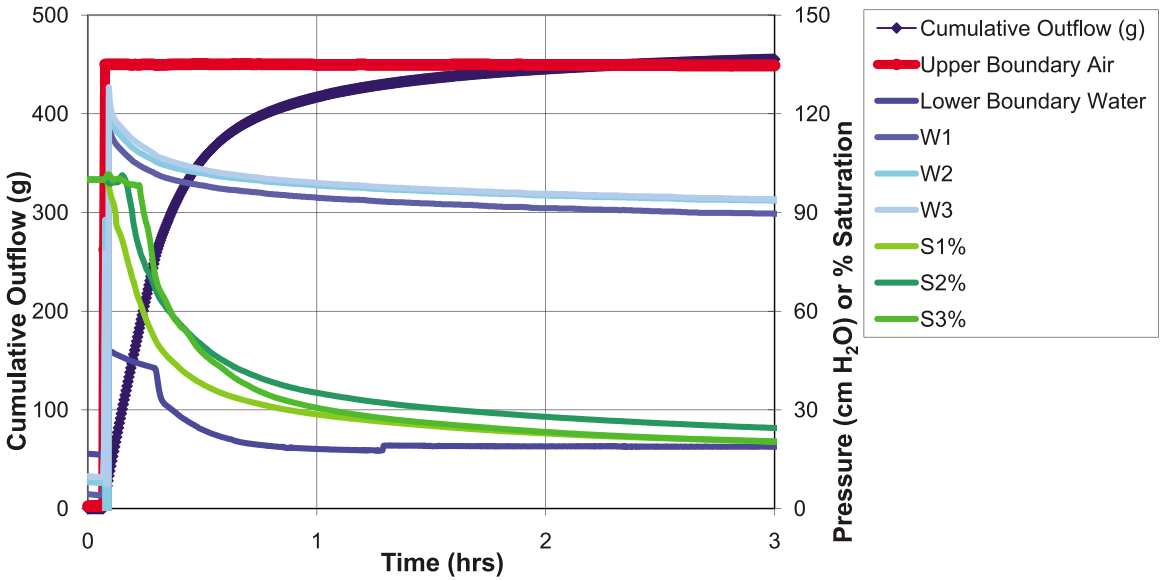

Figure 3. Measured experimental parameter at levels 1, 2 and 3 for F32–F50 dynamic experiment 5 (P_{air} = 135 cm): outflow, tensiometric water pressures (W1, W2 and W3) and saturations (S1, S2 and S3) versus time.

overlap with the static curve suggesting that $P_c^{214\ cm\ water}$ is statistically different than P_c^{static} (Figure 5). Differences in capillary pressure measured under static and dynamic conditions were larger for the F70 sand in comparison to the F32/F50 sand, for the same imposed boundary condition (P_{air} = 135 cm). With the exception of two data points, the 95% confidence intervals of the mean static and dynamic P_c-S_w curves (P_{air} = 135 cm) for the finer F70 sand do not overlap. An analysis of the pressure measurement system (ceramic porous cups + pressure transducers) suggests that any lag in pressure sensor readings (if there are any) would serve to decrease measured capillary pressure below the actual value. Furthermore, the inside volume of the pressure sensor (porous ceramic cup + transducer) was kept as small as possible to maintain high measurement sensitivity. Any lag in water saturation measurements would serve to increase observed dynamic effects in capillary pressure, however, independent tests of the EC-5 probes suggest that they respond immediately to changes in water saturation, as discussed earlier. As a result observed dynamic effects in capillary pressure are not associated with delays in the measurement systems. Increased capillary pressures at higher desaturation rates have also been observed in air-water experiments [e.g., *Topp et al.*, 1967; *Smiles et al.*, 1971; *Vachaud et al.*, 1972; *Stauffer*, 1978; *Wildenschild et al.*, 2001; *Chen et al.*, 2007; *Sakaki et al.*, 2010], and PCE-water experiments [*Berentsen et al.*, 2006; *Bottero et al.*, 2006]. The study of *Sakaki et al.* [2010] reported that capillary pressures, measured under dynamic conditions, fell outside the 95% confidence interval of the static capillary pressures, however, they did not observe

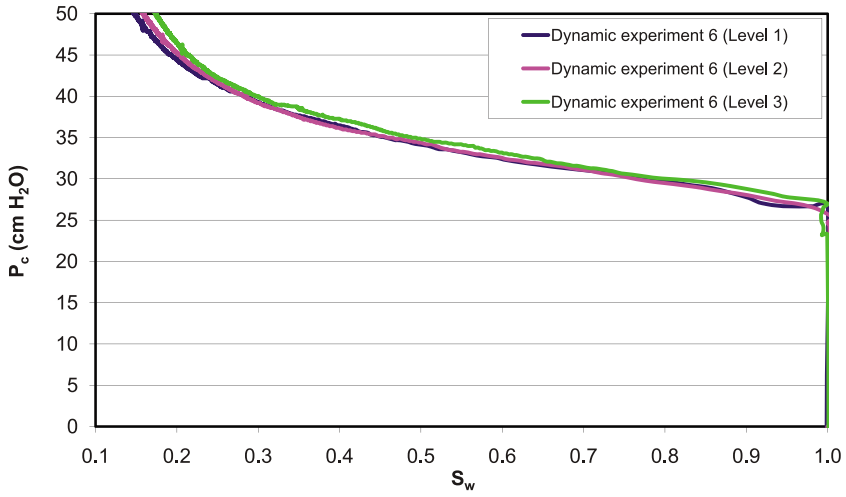

Figure 4. Dynamic P_c-S_w curves measured at three levels (F32/F50 dynamic experiment 6, P_{air} = 214 cm water).

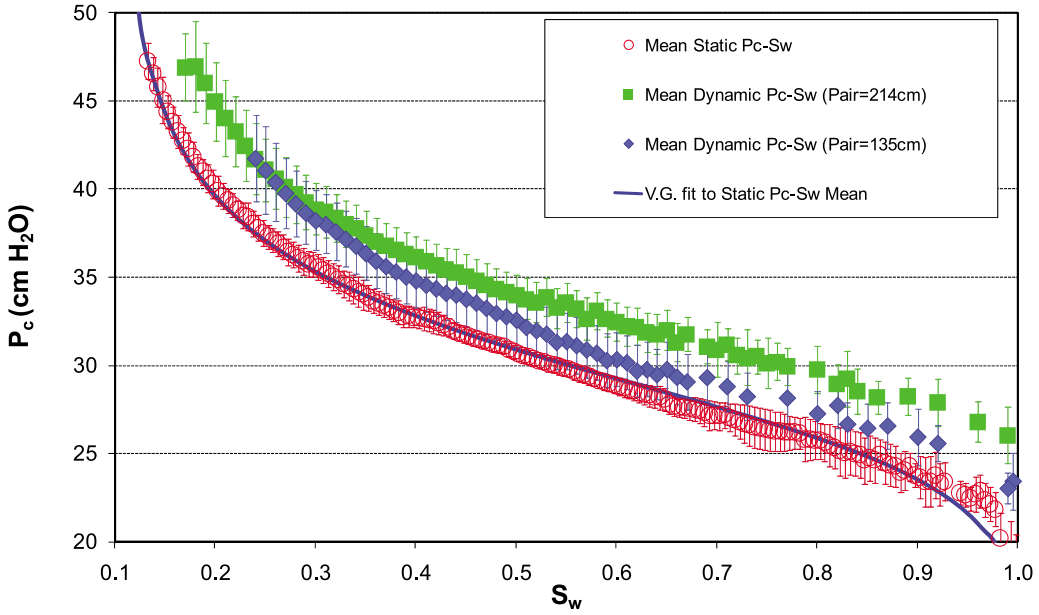

Figure 5. Mean static and dynamic P_c-S_w curves for F32/F50 sand. For dynamic experiments, P_{air} = 135 cm and 214 cm of water. Error bars indicate the 95% confidence intervals about the mean.

increasing differences between static and dynamic P_c with increasing imposed boundary pressure. *Sakaki et al.* [2010] did not compute 95 % confidence intervals for their measured dynamic P_c-S_w curves. The other reported studies did not attempt to quantify statistical differences. Increased capillary pressures with increased rate of desaturation is expected based on thermodynamic considerations [*Kalaydjian*, 1992; *Hassanizadeh and Gray*, 1993] as well as the model of *Barenblatt* [1971]. The apparent dependency of the P_c-S_w relationship on the desaturation rate/boundary condition has been attributed to various physical processes which may account for the observed dynamic or nonequilibrium effects, as discussed in section 1. These phenomena are discussed below in the context of the results observed in this study.

[25] 1. It is known that measured dynamic contact angles differ from the static contact angles [*Friedman*, 1999]. To investigate whether the dynamic contact angle could account for the difference between static and dynamic P_c, the Young-Laplace equation was used to quantify the static contact angle using the ratio of dynamic P_c to static P_c. For example for the

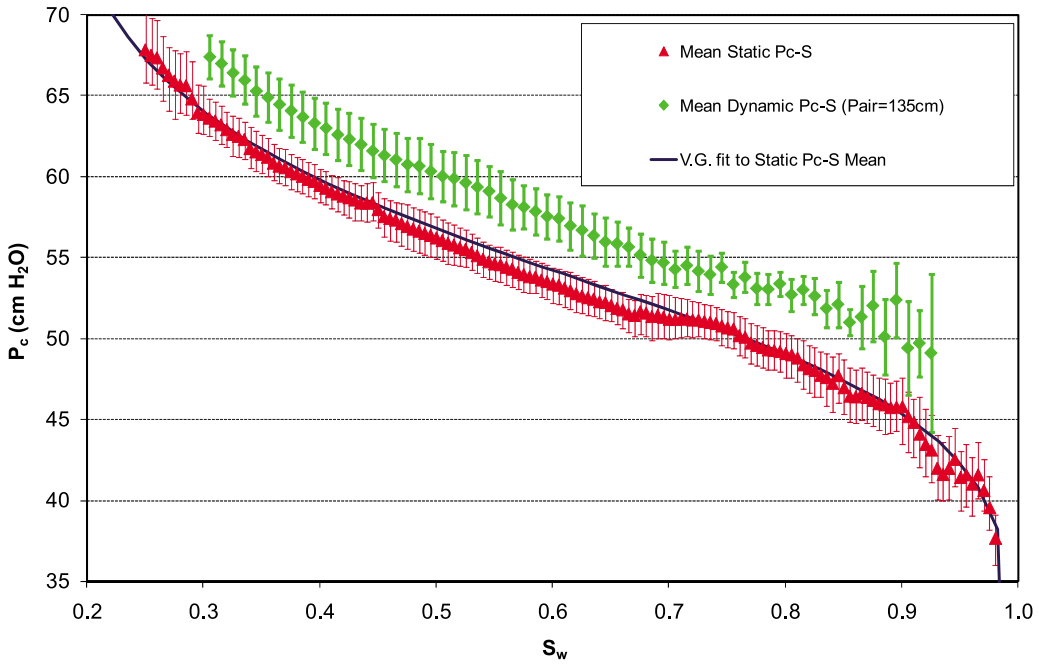

Figure 6. Mean static and dynamic P_c-S_w curves for F70 sand. For dynamic experiments, P_{air} = 135 cm of water. Error bars indicate the 95% confidence intervals about the mean.

Table 3. Comparison of the Normalized Cumulative Outflow at the Onset of Desaturation at Level 1

Experiment Name	$Norm\ Q_c^{eff}$ [a]	Time Air-Water Front Arrives at Level 1 (h)
F32/F50 static experiment 1	0.07	1.79
F32/F50 static experiment 2	0.06	3.17
F32/F50 dynamic experiment 6	0.07	0.12
F32/F50 dynamic experiment 7	0.08	0.10
F32/F50 dynamic experiment 8	0.07	0.13

[a] $Norm Q_c^{eff} = \left(\frac{Q_c}{Q_c^{final}}\right)$ Norm where Q_c is the cumulative outflow Q_c^{final} is the cumulative outflow at the termination of the experiment.

F32/F50 sand if it is assumed that the contact angle, measured under dynamic conditions (P_{air} = 214 cm of water) through the water phase, is 0°, the Young-Laplace equation suggests that the static contact angle would be 46°. This contact angle is larger than would be expected in an air-water-quartz sand system and a contact angle of 0° under dynamic conditions is unlikely. It is therefore unlikely that dynamic contact angles alone result in observed differences in capillary pressure measured under static and dynamic conditions in this study. The ratio of dynamic to capillary forces decreases with saturation, as a result this static contact angle would decrease to more reasonable estimates with decreasing water saturation.

[26] 2. For the F32/F50 drainage experiments, hydrophilic membranes were emplaced at the lower boundary. It has been suggested that large capillary pressure gradients near the membrane in dynamic drainage experiments can result in water drainage first occurring at the outflow end of the column if there is air phase continuity throughout the column [*Wildenschild et al.*, 2001]. In this study, water drained sequentially from levels 1 through 3 in experiments when membranes were used. Furthermore in the F70 drainage experiments no membranes were used and dynamic effects in the measured P_c-S_w relationships were observed. As such membrane effects did not contribute to observed dynamic effects.

[27] 3. In water drainage column experiments, where air enters through the top of the column via small openings that are not large enough to facilitate the movement of air into the column, air pressure within the sample may deviate from atmospheric pressure [*Schultze et al.*, 1997]. In these instances the air phase may expand, resulting in air entrapment [*Wildenschild et al.*, 2001; *Hassanizadeh et al.*, 2002]. To address this concern, drainage was induced by pressurizing the upper air phase boundary in this study, as suggested in the literature [*Hopmans et al.*, 1996]. Air pressure was also quantified at the measurement locations to further confirm that air pressure at the measurement location was equivalent to the imposed upper boundary air pressure. This further confirmed that air entrapment did not result in observed differences between static and dynamic P_c-S_w data.

[28] 4. During dynamic drainage, water may become entrapped in smaller pores as the entry pressure of the larger surrounding pores is exceeded [*Hassanizadeh et al.*, 2002]. The resulting drainage of the larger pores may isolate water in the smaller pores [*Wildenschild et al.*, 2001]. This phenomenon may explain why, during dynamic experiments, water saturation is higher at a given capillary pressure than for static experiments. To assess if water entrapment contributed to observed dynamic effects in capillary pressure the normalized cumulative water outflow at the onset of desaturation at level 1 (depth of 7 cm) are compared for the F32/F50 static and dynamic experiments (P_{air} = 214 cm) (Table 3). If the normalized cumulative water outflow was lower under dynamic conditions, this would suggest that water was in fact entrapped in the region of the column between the upper boundary and level 1. However, the normalized cumulative water outflow at the onset of desaturation at level 1 were similar in the static and dynamic experiments suggesting water entrapment was not a major contributing factor to the observed dynamic effects.

[29] Results from this analysis therefore suggest that (1) both static and dynamic P_c-S_w experiments yield reproducible results, (2) capillary pressures measured under dynamic conditions are statistically different than those measured under static conditions, (3) the magnitude of differences between measured static and dynamic P_c-S_w curves is dependent on both the imposed boundary condition and mean grain size, (4) pore water blockage, water and air entrapment do not likely contribute to observed dynamic capillary pressure effects, and (5) dynamic contact angle does not solely contribute to observed dynamic capillary pressure effects in air/water systems. As discussed in the introduction there are still a number of factors that could contribute to observed dynamic effects that need further study, including measurement scale, grain size distribution, fluid viscosities and interfacial phenomena (e.g., wettability), some of which are investigated below.

3.2. Quantification of Dynamic Coefficient τ

[30] In this section, we calculate the dynamic coefficient τ as a function of water saturation using equation (1) and discuss its magnitude and dependency on grain size and imposed boundary pressure. To quantify the difference between the static and dynamic capillary pressures in equation (1), the static capillary pressure was determined by fitting van Genuchten P_c-S_w [*van Genuchten*, 1980] model parameters to the mean static P_c-S_w data. The van Genuchten model was selected over the Brook and Corey model [*Brooks and Corey*, 1964] due to its better fit to the mean static P_c-S_w data, particularly at higher water saturations. The desaturation rate was determined for each dynamic drainage experiment using a 7 point moving polynomial smoothing routine (i.e., the desaturation rate was averaged over 90 s) [*Golay*, 1972]. The desaturation rate dS_w/dt was only calculated when the difference between two consecutive saturation readings was larger than 0.7% water saturation, the experimental detection limit of the EC-5 soil moisture probes. If changes in two consecutive water saturation readings were less than 0.7% it was assumed that the water saturation did not change. The dynamic coefficient (τ) was quantified using equation (1) at each water saturation where ($P_{NW} - P_W$) was available and when changes in water saturation were greater than the detection limit of the EC-5 probes. Since changes in water saturation decreased below the detection limit of the EC-5 probes as the column became desaturated the dynamic coefficient is generally not reported at lower water saturations. The dynamic experiments were rapid and the measurement frequency of the data logger was 15 s. As a result, quantification of ($P_{NW} - P_W$) at closely spaced water saturations was

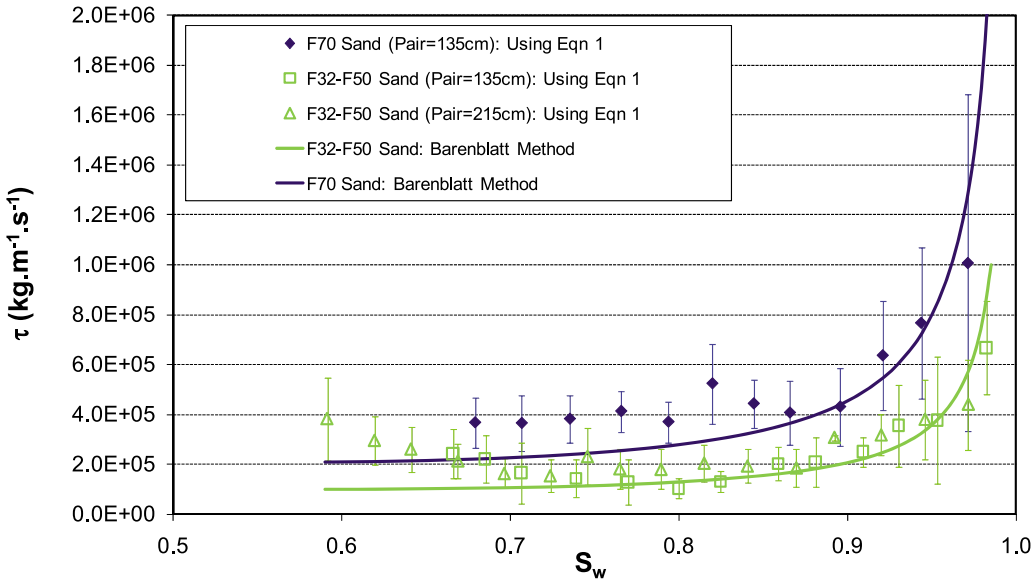

Figure 7. Mean dynamic coefficient (τ) calculated using equation (1) for F70 and F32/F50 sand experiments. The dynamic coefficient calculated using the Barenblatt method (redistribution time = 72 s for the F32/F50 sand and 102 s for the F70 sand) is shown for comparison.

not possible. The dynamic coefficients for each of the dynamic experiments, at a given imposed boundary condition and for a given sand type, were therefore averaged in 0.02 water saturation intervals. This facilitated calculation of 95% confidence intervals about the mean dynamic coefficient for each imposed boundary condition.

[31] The magnitude of averaged τ, shown in Figure 7, is generally largest for completely water saturated conditions and decreases with decreasing water saturation. This is expected from equation (4) as with the VG model, dP_c/dS_w is large at completely water saturated conditions. It should be noted, however, that the error bars are large at completely water saturation conditions. As such, although average values of τ are greater at higher water saturations they are not statistically different than values at lower water saturations. For the F70 sand in this study τ ranges between 10^6 and 3.7×10^5 kg m^{-1} s^{-1} and for the F32/F50 sand τ ranges between 6.7×10^5 and 10^5 kg m^{-1} s^{-1}. This range is consistent with a number of published air-water experimental studies reported in the literature review of *Hassanizadeh et al.* [2002] (i.e., 3×10^4 kg m^{-1} s^{-1} to 5×10^7 kg m^{-1} s^{-1}) as well as a recent study that utilized a field soil in air-water experiments [*Sakaki et al.*, 2010]. For PCE-water-sand systems, a saturation dependent τ of between 10^5 and 10^7 kg m^{-1} s^{-1} has been reported [*O'Carroll et al.*, 2005; *Bottero et al.*, 2006] and an average of 2×10^6 kg m^{-1} s^{-1} has been reported for an oil-water system [*Kalaydjian*, 1992]. Reported values of τ vary over three orders of magnitude in the literature. Further work is therefore needed to determine the factors that contribute to these variations.

[32] The dynamic coefficient was larger in the finer F70 sand in comparison to the coarser F32/F50 sand, with the difference being statistically significant between water saturations of 0.85 and 0.75 (Figure 7). Other studies have suggested that the magnitude of the dynamic coefficient is related to the permeability of the medium [*Stauffer*, 1978; *Manthey et al.*, 2005; *Mirzaei and Das*, 2007] however, to our knowledge this is the first experimental study that has observed that the dynamic coefficient is statistically different for different grain sizes, or equivalently, intrinsic permeability and entry pressure. Using the *Stauffer* [1978] relationship (equation (2)) and the measured soil and fluid properties from this study (Table 1) suggests that τ for the F70 sand should be 11 times larger than for the F32/F50 sand. The maximum and minimum ratio of τ between both sands occurred at $S_w \sim 0.82$ and $S_w \sim 0.67$ respectively (Figure 7). Here the dynamic coefficient was 4 times larger for the F70 sand at $S_w \sim 0.82$ and 1.6 times larger at $S_w \sim 0.67$. The general trend of increasing dynamic coefficient with decreasing intrinsic permeability and increasing entry pressure observed in this study is consistent with that proposed by *Stauffer* [1978], however the magnitude of the ratio for these two sands is different. This analysis has only been conducted for one porous media pair in this study therefore further work is necessary to determine the appropriateness of the relationship proposed by Stauffer for a broader range of porous media types. Comparison of the dynamic coefficient derived from a number of experimental studies suggests that the relationship of *Stauffer* [1978] may not be broadly applicable and further work is necessary to develop a better understanding of the factors impacting the magnitude of the dynamic coefficient [*Hassanizadeh et al.*, 2002].

[33] For the F32/F50 sand used in this study there was no significant difference between τ for the two imposed boundary conditions over the range of water saturations quantified. These different imposed air boundary conditions resulted in different maximum water desaturation rates, as expected (i.e., 1.4×10^{-3} s^{-1} and 2.4×10^{-3} s^{-1} for P_{air} = 135 cm water and P_{air} = 214 cm water, respectively). This may suggest that division of dP_c by dS_w/dt at a given saturation, as defined in equation (1), remains similar regardless of the imposed boundary condition. These results are consistent with the heterogeneous sand simulation results of *Manthey et al.* [2005] that found that under three different

desaturation regimes there was no pronounced difference between τ when water saturation was larger than 0.7. In their study, however, τ increased with applied pressure step size at lower water saturations. In this study τ was not quantified below a water saturation of 0.6 because the water saturation change over the measurement time interval was less than the detection limit of the EC-5 soil moisture probe at lower water saturations.

3.3. Assessment of Controlling Forces and Determination of Redistribution Time

[34] In order to determine the conditions when dynamic effects become important, *Manthey et al.* [2008] carried out a dimensional analysis of the two-phase mass balance equations. Inclusion of the extended P_c-S_w relationship (i.e., including equation (1) in this analysis) yielded two new dimensionless numbers that could be used to compare the magnitude of dynamic capillary forces to both viscous and equilibrium capillary forces. These numbers are calculated here to assess the importance of the magnitude of dynamic capillary forces in this study. The dimensionless dynamic number (*Dy*), developed through dimensionless analysis of the nonwetting phase mass balance equation, relates the magnitude of dynamic capillary forces to viscous forces [*Dahle et al.*, 2005; *Manthey et al.*, 2008]:

$$Dy = \frac{k\tau}{\mu_w l_c^2 \phi} \tag{5}$$

where μ_w is the viscosity of the wetting phase and l_c is a characteristic length. In this study l_c is taken as the measurement range of the EC-5 soil moisture probes and the sampling range over which the desaturation rate was quantified (approximately 1 cm for desaturation with the probe alignment adopted in this study) [*Limsuwat et al.*, 2009]. *Manthey et al.* [2008] investigated the use of system length, front width length and pore diameter as appropriate characteristic lengths and suggested that the front width is most appropriate. A *DyC* number, relating the magnitude of dynamic capillary forces to equilibrium capillary forces, has also been proposed:

$$DyC = \frac{u_c \tau}{P_{cc} l_c \phi} \tag{6}$$

where u_c is a characteristic velocity and P_{cc} is a characteristic capillary pressure, in this study taken as the entry pressure fit using the Brooks-Corey relationship. u_c/l_c was assumed to be equivalent to the desaturation rate in this study. In these calculations, maximum observed desaturation rates of 1.4×10^{-3} s^{-1} and 2.4×10^{-3} s^{-1} were used for the F32/F50 sand at imposed boundary conditions of 135 cm water and 214 cm water, respectively and 2.1×10^{-3} s^{-1} for the F70 sand at an imposed boundary condition of 135 cm water. The dynamic number was *Dy* = 968 for the F32/F50 sand and 410 for the F70 sand and the *DyC* number was 1.3 and 2.3 for the F32/F50 sand at the imposed boundary conditions 135 cm water and 214 cm water, respectively and 1.4 for the F70 sand. Note that the dynamic number is not a function of the desaturation rate. This analysis suggests that dynamic capillary forces were larger than both viscous and equilibrium capillary forces in this study, however the dynamic capillary forces were on the same order as the equilibrium capillary forces. This is consistent with the observed capillary pressure/saturation curves which were statistically different under dynamic and static conditions however the magnitude of these differences were generally 10% to 15% of the entry pressure of the two sands in this study.

[35] The work of *Barenblatt* [1971] suggests that observed dynamic effects are due to a finite time required for pore fluids to redistribute in the pore space. The redistribution times are calculated here using the dynamic coefficient determined by minimizing the RMSE between the dynamic coefficients estimated using equations (1) and (4) (Figure 7), facilitating a comparison of the two theories. Redistribution times were 72 s for the F32/F50 sand and 102 s for the F70 sand, suggesting that a finite and a readily observable time is required for the pore fluids to redistribute in these systems. The redistribution time, which is largely independent of saturation, is larger for the F70 sand, consistent with the larger reported dynamic coefficients. Larger redistribution times may therefore be required in porous media with a smaller pore structure. These values are smaller than the 509 s redistribution time reported by *Sakaki et al.* [2010] for primary water drainage in an air-water system. They utilized a similar experimental apparatus with a mean grain size of 0.3 mm, which is between that of the F32/F50 and F70 sands used here, however their sand had a larger uniformity coefficient. *Sakaki et al.* [2010] also utilized the Brooks-Corey model to obtain the slope of the P_c-S_w relationships, as opposed to the van Genuchten model used in this study, and they utilized dynamic coefficients at lower water saturations in their fitting routine, where the dynamic coefficients were largest. As suggested by equation 4, the shape of the measured τ-S_w relationships in Figure 7 seems to be largely controlled by the slope of P_c-S_w relationships. All of these factors could have contributed to the larger reported redistribution time of *Sakaki et al.* [2010].

3.4. Upscaling τ for Larger Systems

[36] As discussed in section 1 numerical and theoretical studies have suggested that τ is proportional to the square of the length scale when pressures and saturations are averaged over the length scale [*Dahle et al.*, 2005; *Manthey et al.*, 2005; *Nordbotten et al.*, 2008]. To investigate the impact of scale on the magnitude of τ, fluid pressures and saturations at each measurement location (with a representative sampling thickness of the sensor = ~1 cm) were upscaled to lengths of 6 cm or 9 cm using the volume averaging technique used by *Manthey et al.* [2005]. For F32/F50 dynamic experiment 4 (P_{air} = 135 cm) and F32/F50 dynamic experiment 7 (P_{air} = 214 cm), point-measured local pressure and saturation measurements (levels 2 and 3) were averaged over 6 cm (i.e., two 3 cm-thick layers). Measurements at all three levels were used to average over a 9 cm interval (i.e., three 3 cm thick layers) for F32/F50 dynamic experiment 6 (P_{air} = 214 cm) and F70 dynamic experiments 1, 2 and 3 (P_{air} = 135 cm). For the other F32/F50 dynamic experiments, the averaging technique could not be applied because both pressure and saturation data from multiple levels were not available. The values of τ averaged over 6 and 9 cm for both sand systems were very similar to the point measurements (Figure 8 for F35/F50 sand dynamic experiment 6 and Figure 9 for F70 sand dynamic experiment 1, other results not shown). Upscaled dynamic coefficients were similar to the point

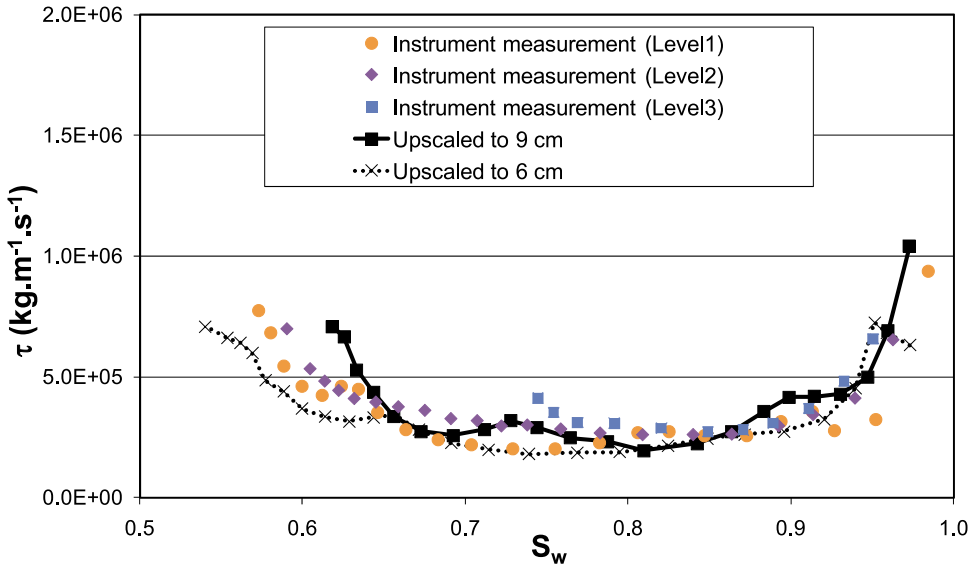

Figure 8. Point measured and upscaled τ as a function of S_w (F32/F50 dynamic experiment 6).

measurements since the magnitude of differences in static and dynamic capillary pressure did not increase with scale nor did the desaturation rate decrease with increasing scale. These observations suggest that column-scale upscaling using the method of *Manthey et al.* [2005] (from a 1 cm local measurement to 9 cm) did not affect the magnitude of τ under the conditions considered in this study (i.e., uniform/homogeneous sand, air-water fluids, and boundary conditions). The study of *Manthey et al.* [2005] utilized different fluid pairs (PCE-water) and a heterogeneous domain ranging from 3 to 100 cm in size. In their study τ increased by approximately 3 orders of magnitude with a 30 fold increase in averaging scale (i.e., from 3 to 100 cm), and by one order of magnitude when the averaging scale increased from 3 cm to 12 cm. Although *Manthey et al.* [2005] used the PCE/water fluid pair the 3 cm and 12 cm averaging scales are similar to that used in this study. It is possible that with the conditions of this study and averaging over a larger column length would lead to increases in the dynamic coefficient. Further investigation is necessary to determine whether or not there is a threshold scaling size for which the averaged τ is significantly affected.

4. Conclusions

[37] In this study, a number of capillary pressure–saturation (P_c-S_w) relationships were measured at different desaturation rates to determine if the relationships depend on desaturation rate, as have been suggested in modeling, theoretical and experimental studies. A number of replicate air-water primary drainage experiments were conducted using two sands with different mean grain sizes (F32/F50 and F70 sands), facilitating statistical comparison of the static and dynamic P_c-S_w relationships. The 95 % confidence intervals of the measured P_c-S_w data (both static and dynamic) showed that the P_c-S_w relationships under fast drainage rates were statistically different than those measured under static conditions for both F32/F50 and F70 sands, consistent with thermodynamic theory. Although the magnitude of differences between capillary pressure, measured under static and dynamic conditions increased with increased imposed boundary condition, pore water blockage, water and air entrapment do not likely contribute to observed dynamic capillary pressure effects. Finally, dynamic contact angle could be a contributing factor but it is does not solely lead to observed dynamic effects in air/water systems.

[38] The dynamic coefficient τ quantified using equation (1) showed that averaged values of τ vary with S_w and the shape of τ-S_w appears to be largely controlled by the slope of the P_c-S_w relationship. However, due to the large confidence intervals for τ near completely water saturated conditions, the averaged τ values at lower S_w lie roughly at the lower bound of the confidence intervals for τ near completely water saturated conditions, i.e., τ values are not statistically different at different water saturations. This suggests that the assumption of a constant τ may also be appropriate. A constant τ model could simplify the implementation of dynamic effects in capillary pressure in a numerical model when modeling unsaturated flow under conditions similar to

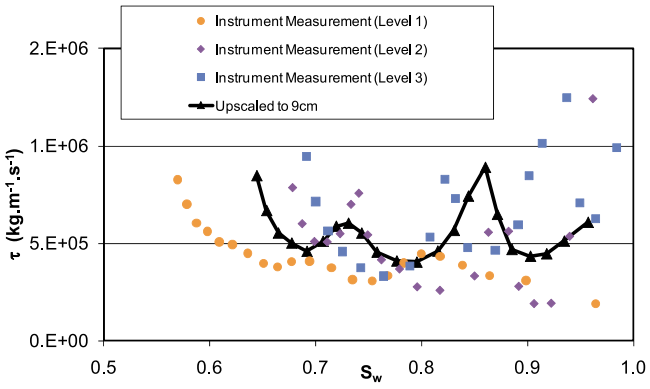

Figure 9. Point measured and upscaled τ as a function of S_w (F70 dynamic experiment 1).

those presented here. Also shown is that the magnitude of τ is consistent with other studies and that τ is dependent on porous media mean grain size (i.e., larger τ for finer soil) but not on the desaturation rate. Finally the dynamic coefficient was upscaled from local point measurements to the column scale. Within the scale that was considered (i.e., ten-fold), the upscaled dynamic coefficients were the same as the point measurements. Additional work is required to investigate other factors that could contribute to observed dynamic effects, including fluid viscosities and interfacial phenomena (e.g., wettability). Furthermore, study is needed to investigate what the implications of dynamic effects would be for common field scenarios where rapid changes in fluid saturations are induced (e.g., air sparging for site remediation, CO_2 sequestration or enhanced oil recovery). Results from this study would suggest that the inclusion of dynamic effects in capillary pressure should be considered when fluid saturations change rapidly.

[39] **Acknowledgments.** This research was supported by Natural Sciences and Engineering Research Council (NSERC) of Canada and Canadian Foundation for Innovation grants. Such support does not indicate endorsement by any sponsor. The authors would also like to thank Michael Celia for helpful advice.

References

Barenblatt, G. I. (1971), Filtration of two nonmixing fluids in a homogeneous porous medium, *Izv. Akad. Nauk SSSR, Mekh. Zhidk. Gaza*, *5*, 857–864.

Barenblatt, G. I., T. W. Patzek, and D. B. Silin (2003), The mathematical model of nonequilibrium effects in water-oil displacement, *SPE J.*, *8*(4), 409–416, doi:10.2118/87329-PA.

Berentsen, C., S. M. Hassanizadeh, A. Bezuijen, and O. Oung (2006), Modelling of two-phase flow in porous media including non-equilibrium capillary pressure effects, in *Proceedings of the XVI International Conference on Computational Methods in Water Resources*, edited by P. J. Binning et al., 11 pp., Tech. Univ. of Denmark, Copenhagen, Denmark. (Available at http://proceedings.cmwr-xvi.org/contributionDisplay.py?contribId=329&sessionId=7&confId=a051)

Bottero, S., S. M. Hassanizadeh, P. J. Kleingeld, and A. Bezuijen (2006), Experimental study of dynamic capillary pressure effect in two-phase flow in porous media, in *Proceedings of the XVI International Conference on Computational Methods in Water Resources*, edited by P. J. Binning et al., 7 pp., Tech. Univ. of Denmark, Copenhagen, Denmark. (Available at http://proceedings.cmwr-xvi.org/contributionDisplay.py?contribId=343&sessionId=9&confId=a051)

Brooks, R. H., and A. T. Corey (1964), Hydraulic properties of porous media, *Hydrol. Pap. 3*, 27 pp., Colo. State Univ., Fort Collins.

Chen, L. X., G. A. Miller, and T. C. G. Kibbey (2007), Rapid pseudo-static measurement of hysteretic capillary pressure-saturation relationships in unconsolidated porous media, *Geotech. Test. J.*, *30*(6), 474–483.

Czarnomski, N., G. W. Moore, T. G. Pypker, J. Licata, and B. J. Bond (2005), Precision and accuracy of three alternative instruments for measuring soil water content in two forest soils of the Pacific Northwest, *Can. J. For. Res.*, *35*(8), 1867–1876, doi:10.1139/x05-121.

Dahle, H. K., M. A. Celia, and S. M. Hassanizadeh (2005), Bundle-of-tubes model for calculating dynamic effects in the capillary-pressure-saturation relationship, *Transp. Porous Media*, *58*(1–2), 5–22, doi:10.1007/s11242-004-5466-4.

Das, D. B., R. Gauldie, and M. Mirzaei (2007), Dynamic effects for two-phase flow in porous media: Fluid property effects, *AIChE J.*, *53*(10), 2505–2520, doi:10.1002/aic.11292.

Friedman, S. P. (1999), Dynamic contact angle explanation of flow rate-dependent saturation-pressure relationships during transient liquid flow in unsaturated porous media, *J. Adhes. Sci. Technol.*, *13*(12), 1495–1518, doi:10.1163/156856199X00613.

Golay, M. J. E. (1972), Smoothing of data by least-squares procedures and by filtering, *IEEE Trans. Comput.*, *21*(3), 299–301, doi:10.1109/TC.1972.5008953.

Hassanizadeh, S. M., and W. G. Gray (1990), Mechanics and thermodynamics of multiphase flow in porous media including interphase boundaries, *Adv. Water Resour.*, *13*(4), 169–186, doi:10.1016/0309-1708(90)90040-B.

Hassanizadeh, S. M., and W. G. Gray (1993), Thermodynamic basis of capillary-pressure in porous media, *Water Resour. Res.*, *29*(10), 3389–3405, doi:10.1029/93WR01495.

Hassanizadeh, S. M., M. A. Celia, and H. K. Dahle (2002), Dynamic effect in the capillary pressure-saturation relationship and its impacts on unsaturated flow, *Vadose Zone J.*, *1*, 38–57, doi:10.2113/1.1.38.

Hopmans, J. W., M. E. Grismer, J. Chen, and Y. P. Liu (1996), Parameter estimation of two-fluid capillary pressure-saturation and permeability functions, *EPA/600/R98/046*, 97 pp., EPA, Cincinnati, Ohio.

Juanes, R. (2008), Nonequilibrium effects in models of three-phase flow in porous media, *Adv. Water Resour.*, *31*(4), 661–673, doi:10.1016/j.advwatres.2007.12.005.

Kalaydjian, F. (1992), Dynamic capillary pressure curve for water/oil displacement in porous media: Theory vs. experiment, *24813-MS*, 16 pp., Soc. of Petrol. Eng., Richardson, Tex.

Klute, A., and C. Dirksen (1986), Hydraulic conductivity and diffusivity: Laboratory methods, in *Methods of Soil Analysis: Part 1*, edited by A. Klute, pp. 687–734, Am. Soc. of Agron., Madison, Wis.

Limsuwat, A., T. Sakaki, and T. H. Illangasekare (2009), Experimental quantification of bulk sampling volume of ECH_2O soil moisture sensors, in *29th Annual American Geophysical Union Hydrology Days*, edited by J. A. Ramirez, pp. 39–45, Colo. State Univ., Fort Collins.

Manthey, S. (2006), Two-phase flow processes with dynamic effects in porous media—Parameter estimation and simulation, dissertation, 139 pp., Univ. of Stuttgart, Stuttgart, Germany.

Manthey, S., S. M. Hassanizadeh, and R. Helmig (2005), Macro-scale dynamic effects in homogeneous and heterogeneous porous media, *Transp. Porous Media*, *58*(1–2), 121–145, doi:10.1007/s11242-004-5472-6.

Manthey, S., S. M. Hassanizadeh, R. Helmig, and R. Hilfer (2008), Dimensional analysis of two-phase flow including a rate-dependent capillary pressure-saturation relationship, *Adv. Water Resour.*, *31*(9), 1137–1150, doi:10.1016/j.advwatres.2008.01.021.

Mirzaei, M., and D. B. Das (2007), Dynamic effects in capillary pressure-saturations relationships for two-phase flow in 3D porous media: Implications of micro-heterogeneities, *Chem. Eng. Sci.*, *62*(7), 1927–1947, doi:10.1016/j.ces.2006.12.039.

Nordbotten, J. M., M. A. Celia, H. K. Dahle, and S. M. Hassanizadeh (2008), On the definition of macroscale pressure for multiphase flow in porous media, *Water Resour. Res.*, *44*, W06S02, doi:10.1029/2006WR005715.

O'Carroll, D. M., T. J. Phelan, and L. M. Abriola (2005), Exploring dynamic effects in capillary pressure in multistep outflow experiments, *Water Resour. Res.*, *41*, W11419, doi:10.1029/2005WR004010.

Sah, A., H. L. Castricum, A. Bliek, D. H. A. Blank, and J. E. ten Elshof (2004), Hydrophobic modification of γ-alumina membranes with organochlorosilanes, *J. Membr. Sci.*, *243*(1–2), 125–132, doi:10.1016/j.memsci.2004.05.031.

Sakaki, T., A. Limsuwat, K. M. Smits, and T. H. Illangasekare (2008), Empirical two-point α-mixing model for calibrating the ECH_2O EC-5 soil moisture sensor in sands, *Water Resour. Res.*, *44*, W00D08, doi:10.1029/2008WR006870.

Sakaki, T., D. M. O'Carroll, and T. H. Illangasekare (2010), Direct quantification of dynamic effects in capillary pressure for drainage-wetting cycles, *Vadose Zone J.*, *9*, 424–437, doi:10.2136/vzj2009.0105.

Schultze, B., O. Ippisch, B. Huwe, and W. Durner (1997), Dynamic non-equilibrium during unsaturated water flow, in *Proceedings of the International Workshop on Characterization and Measurement of the Hydraulic Properties of Unsaturated Porous Media*, edited by M. T. van Genuchten, F. J. Leij, and L. Wu, pp. 877–892, Univ. of Calif., Riverside.

Smiles, D. E., G. Vachaud, and M. Vauclin (1971), Test of uniqueness of soil moisture characteristic during transient nonhysteretic flow of water in a rigid soil, *Soil Sci. Soc. Am. Proc.*, *35*, 534–539.

Stauffer, F. (1978), Time dependence of the relations between capillary pressure, water content and conductivity during drainage of porous media, paper presented at Symposium on Scale Effects in Porous Media, IAHR, Thessaloniki, Greece.

Topp, G. C., A. Klute, and D. B. Peters (1967), Comparison of water content-pressure head data obtained by equilibrium steady-state and unsteady-state methods, *Soil Sci. Soc. Am. Proc.*, *31*, 312–314.

Vachaud, G., M. Vauclin, and M. Wakil (1972), Study of uniqueness of soil-moisture characteristic during desorption by vertical drainage, *Soil Sci. Soc. Am. Proc.*, *36*, 531–532.

van Genuchten, M. T. (1980), Closed-form equation for predicting the hydraulic conductivity of unsaturated soils, *Soil Sci. Soc. Am. J.*, *44*, 892–898.

Vogel, H.-J., A. Samouelian, and O. Ippisch (2008), Multi-step and two-step experiments in heterogeneous porous media to evaluate the relevance of dynamic effects, *Adv. Water Res.*, *31*(1), 181–188.

Wildenschild, D., J. W. Hopmans, and J. Simunek (2001), Flow rate dependence of soil hydraulic characteristics, *Soil Sci. Soc. Am. J.*, *65*, 35–48.

G. Camps-Roach, T. A. Newson, and D. M. O'Carroll, Department of Civil and Environmental Engineering, University of Western Ontario, London, ON N6A 5B9, Canada. (docarroll@eng.uwo.ca)

T. H. Illangasekare and T. Sakaki, Center for Experimental Study of Subsurface Environmental Processes, Colorado School of Mines, Golden, CO 80401, USA.